Journal of Agrometeorology

ISSN : 0972-1665 (print), 2583-2980 (online)
Vol. No. 26 (4) : 401-410 (December - 2024)
https://doi.org/10.54386/jam.v26i4.2665
https://journal.agrimetassociation.org/index.php/jam

Research Paper

Comprehensive air quality analysis in Karbala: Investigating the relationships between meteorological factors and pollutants across different landscapes

HAYDER H. ALI[*1], BASIM I. WAHAB[1] and HAYDER M. ABDUL AL-HMEED[2]

[1]*Department of Atmospheric Science, College of Science, University of Mustansiriyah, Baghdad, Iraq.*
[2]*Department of Environment Engineering, College of Engineering, University of Baghdad, Bagdad, Iraq*
[*]*Corresponding author E-mail: hayder@uomustansiriyah.edu.iq*

ABSTRACT

Atmospheric elements interact with pollutants in complex, multidimensional ways, affecting air quality. Understanding these relationships requires a comprehensive analysis of time-series weather and pollutant data which has a negative or positive impact on the ecosystem and human health. This study examines the relationships between meteorological factors and air pollutants in different landscapes (agricultural, park, desert and industrial) of Karbala, Iraq, using data from January 2021 to June 2024. Principal component analysis (PCA) revealed that photochemical smog (45-46%), particulate matter (20-22%), and meteorological effects on particulates (14-16%) are the main factors influencing air pollution. $PM_{2.5}$ was the dominant pollutant, impacting air quality on 84-88% of days, followed by ozone on 12-16%. Winter showed the best air quality, while summer had no "Good" days. Among the four areas studied, the desert suburb had the cleanest air, and the industrial area the most polluted. These findings offer crucial insights for air quality management in the region.

Keywords: Air Quality Index, Pollutants, Principal component analysis (PCA), Polar plot. Weather parameters, Agricultural area

Air pollution is a significant global concern due to its severe impacts on ecosystems and human health, as well as its role in altering the global climate (Abdullatif *et al.,* 2021; Yaseen and Abdulkareem, 2022). Urban areas are particularly affected by high levels of air pollution, primarily from anthropogenic activities like fossil fuel combustion in transportation and industry. Additionally, wind-borne particulate matter further degrades urban air quality. Pollutants such as O_3, NO_2, SO_2, CO, $PM_{2.5}$, and PM_{10} can persist in the atmosphere for hours to days, with their dispersion influenced by meteorological factors (Jayamurugan *et al.,* 2013; Anad *et al.,* 2022; Taghizadeh *et al.,* 2023). Exposure to these pollutants is linked to respiratory and psychological disorders, including asthma (Byrwa-Hill *et al.,* 2020), nasal and throat irritation, hypertension, atherosclerosis, acute coronary syndrome, ischemic stroke, and arrhythmias. Various indices have been developed to quantify the effect of climatic parameters on the discomfort levels (Pandey, 2018).

Emerging research suggests a connection between air pollution and cognitive decline, with higher dementia risk observed in individuals exposed to elevated $PM_{2.5}$ levels also risk of lung and other cancers. Rapid urbanization, population growth, and vehicle proliferation, particularly in developing countries like Iraq, have exacerbated air pollution problems (Jadem *et al.,* 2023). In addition, meteorological factors are the main drivers that affect the concentrations of various air pollutants and overall air quality such as temperature, solar radiation, wind, and precipitation. Karbala, due to its strategic location and religious significance, has experienced rapid development, impacting air quality.

The air quality index (AQI) is widely used by governments and organizations to inform the public about air quality and its health implications. These assessments rely on continuous monitoring of pollutants, which are integrated into AQI models (Gayer *et al.,* 2018). AQI has been closely related to discomfort indices (Mohamed *et al.,* 2023). Scientists use many statistical techniques and predictive models to demonstrate the relationship between different atmospheric parameters such as correlation coefficients,

Article info - DOI: *https://doi.org/10.54386/jam.v26i4.2665*
Received: 17 July 2024; Accepted: 2 September 2024 ; Published online : 01 December 2024

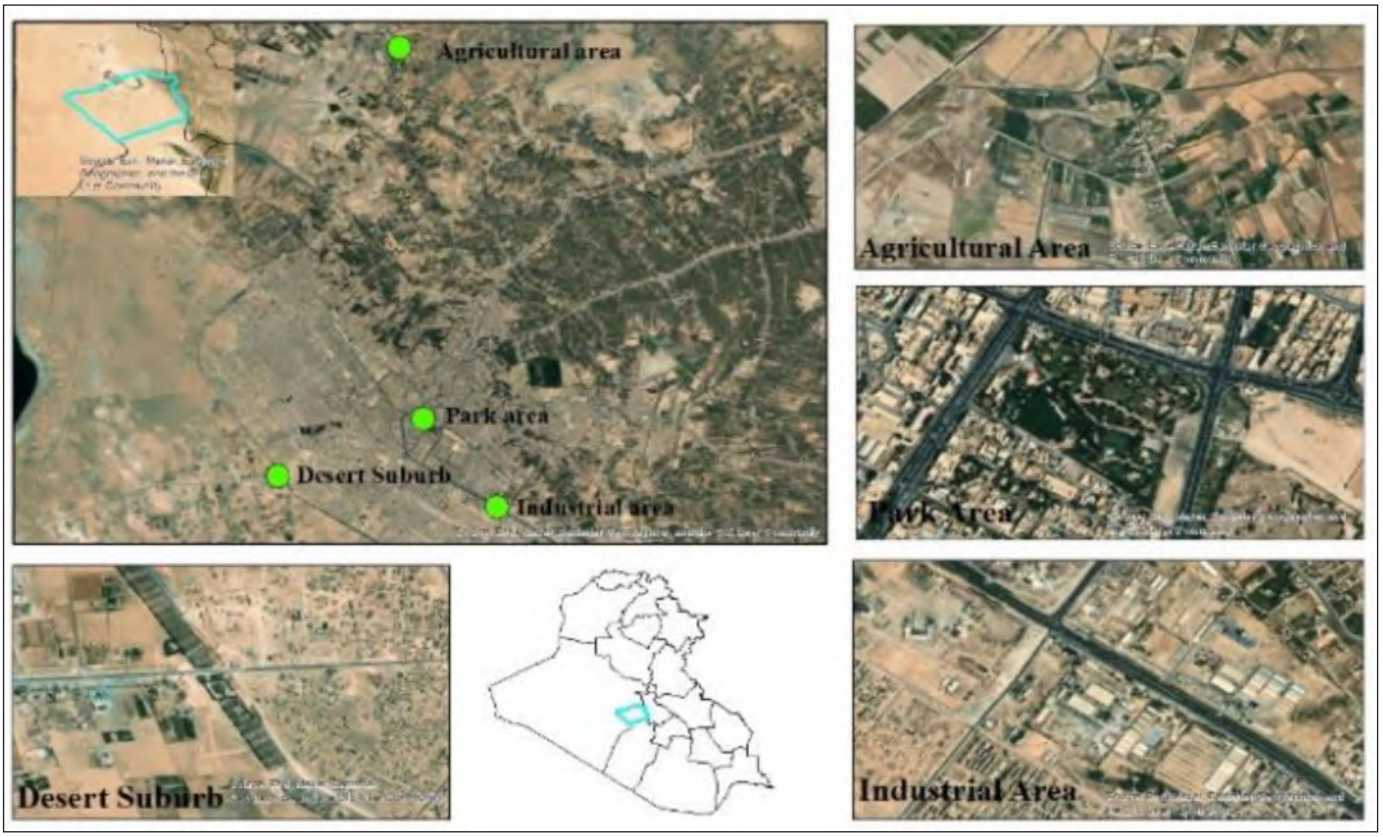

Fig. 1: Study area

linear and multiple regression, principal component analysis, and others. Zuśka *et al.,* (2019) used principal component analysis (PCA) to analyze the influence of meteorological factors on PM_{10} concentrations in a mountain valley over 10 years.

The study found that temperature significantly influenced PM_{10} levels across most seasons, with wind speed, humidity, atmospheric pressure, and precipitation also contributing. High PM_{10} concentrations in winter were associated with anticyclonic wedge conditions. Shihab (2021) analysed the AQI in Mosul and found that AQI levels ranged from moderate to unhealthy for sensitive groups, with PM_{10} being the primary contributor, and noted seasonal variations in AQI. Birinci *et al.,* (2023) studied the impact of long-range dust transport on PM concentrations at Turkish airports, identifying 163 dust episodes, with significant contributions from North Africa (17%) and the Mediterranean (12%). This underscores the importance of considering transboundary dust sources in air quality assessments. The present research aims to analyze the relationship between various meteorological factors and primary air quality index (AQI) pollutants, as well as to evaluate the daily AQI for selected areas for January 2021 - June 2024.

MATERIALS AND METHODS

Study area

Karbala governorate, located approximately 100 km southwest of Baghdad, Iraq, is characterized by a subtropical semi-arid climate. It covers an area of 52 km^2 and is situated at an elevation of 32 meters above sea level. The region is bordered by desert and agricultural lands and is in proximity to the Euphrates and Husseinya rivers. Karbala is a significant religious and tourist center in Iraq, renowned for its Islamic heritage sites. The governorate has an estimated population of approximately 1.35 million people (Al-Samarrai and Al-Jiboori, 2022). Fig. 1 shows study area, Agricultural area (Lat 32.72 ^{0}N, Long 44.00 ^{0}E), Park area (Lat 32.60 ^{0}N, Long 44.03 ^{0}E), Desert suburb (Lat 32.58 ^{0}N, Long 43.98 ^{0}E) and Industrial area (Lat 32.57 ^{0}N, Long 44.05 ^{0}E).

Dataset sources

The Copernicus Atmosphere Monitoring Service (CAMS) provides continuous data on atmospheric composition, offering current conditions, forecasts, and retrospective analyses for recent years. This service supports applications in health, environmental monitoring, renewable energy, meteorology, and climatology. Data for air pollutants (tropospheric ozone O_3, nitrogen dioxide (NO_2), sulfur dioxide (SO_2), carbon monoxide (CO), particulate matter ($PM_{2.5}$ and PM_{10}) were sourced from Copernicus at: https://ads.atmosphere.copernicus.eu/cdsapp#!/dataset/cams-europe-air-quality-forecasts?tab=form. Meteorological data, including temperature (T), relative humidity (RH), All sky surface shortwave downward irradiance SWDI (solar radiation), wind speed (WS), and wind direction (WD), were obtained from NASA's Prediction of Worldwide Energy Resources (POWER), Agroclimatology data at: https://power.larc.nasa.gov/data-access-viewer/. All data cover the period from January 2021 to June 2024.

Principal component analysis (PCA)

Principal component analysis (PCA) is a statistical method used to reduce the dimensionality of data by transforming

Table 1: Categories of air quality index (AQI)

AQI	Descriptor	Colour
0 to 50	Good	Green
51 to 100	Moderate	Yellow
101 to 150	Unhealthy for sensitive groups	Orange
151 to 200	Unhealthy	Red
201 to 300	Very unhealthy	Purple
301 to 500	Hazardous	Maroon

Table 2: Eigenvalue, variance and cumulative of principal components

Location	**Agricultural area**			**Park area**		
Principal component	PC1	PC2	PC3	PC1	PC2	PC3
Eigenvalue	5.04837	2.39164	1.59244	5.07481	2.37673	1.57854
Variance (%)	45.89%	21.74%	14.48%	46.13%	21.61%	14.35%
Cumulative (%)		82.11%			82.09%	
Location	**Desert suburb**			**Industrial area**		
Principal component	PC1	PC2	PC3	PC1	PC2	PC3
Eigenvalue	5.00748	2.3276	1.68239	5.02414	2.25741	1.74591
Variance (%)	45.52%	21.16%	15.29%	45.67%	20.52%	15.87%
Cumulative (%)		81.98%			82.07%	

the correlation relationships between them. PCA aids in identifying groups of uncorrelated variables, thereby facilitating the analysis of complex datasets (Zuśka *et al.,* 2019).

Air quality index (AQI)

The primary purpose of the air quality index (AQI) is to convert the measured concentrations of various air pollutants into a single, standardized numerical value through an appropriate aggregation method. Ideally, each index value should accurately represent both the actual and perceived air quality for a specific time period. Air quality indices are designed to standardize and consolidate air pollution data, making it easier to compare different conditions and meet the public's demand for reliable and easily understandable information. Table 1 presents the categories of the air quality index as defined by the U.S. Environmental Protection Agency (EPA).

Sub-indices are computed using the equation below (Shihab, 2021);

$$I_P = \frac{I_{Hi} - I_{Lo}}{BP_{Hi} - BP_{Lo}} (CP - BP_{Lo}) + I_{Lo} \quad (1)$$

Where (I_p) is index for pollutant *p*, (C_p) is truncated concentration of pollutant p, (BP_{HI}) is concentration breakpoint greater than or equal to C_p, (BP_{Lo}) is concentration breakpoint less than or equal to C_p, (I_{Hi}) is AQI value corresponding to BP_{HI}, (I_{Lo}) is AQI value corresponding to BP_{Lo}. These breakpoints can be found in (Technical Assistance Document for the Reporting of Daily Air Quality – the Air Quality Index (AQI)) in https://www.airnow.gov/publications/air-quality-index/technical-assistance-document-for-reporting-the-daily-aqi/.

The value of the highest sub-indices AQI is considered the AQI of the site (eq. 2) (Shihab, 2021).

$$AQI = Max(I\_a, I\_b, I\_c, \ldots, In) \quad (2)$$

RESULTS AND DISSECTIONS

Analysis the relationship of meteorological and pollutants by PCA

Principal components analysis (PCA) was conducted on the concentrations of selected air pollutants and meteorological parameters. The analysis identified five principal components, with the first three components having eigenvalues greater than 1, in accordance with the Kaiser criterion. In PCA, the proportion of variance explained by each principal component is represented by the square of the factor loadings, which can be interpreted as the coefficient of determination. This coefficient reflects the proportion of the variance in air pollutant concentrations and meteorological factors that can be attributed to their mutual influence. Examination of the eigenvalues in the correlation matrix (Table 2) indicated that the first three principal components accounted for approximately 81.98% to 82.11% of the total variance, highlighting their significance in explaining the dataset's variability.

PC1, accounting for 45-46% of the total variance in all regions, predominantly characterizes photochemical smog formation. It exhibits height positive loadings for ozone (0.39-0.40), temperature (0.33-0.34), and solar radiation (SWDI: 0.35-0.36), coupled with negative loadings for primary pollutants including NO_2 (-0.35 to -0.36), SO_2 (-0.32 to -0.33), CO (-0.37 to -0.39) and RH (-0.31 to -0.32). The positive correlations with temperature and solar radiation (SWDI) underscore the critical role of solar light in driving photochemical reactions (Wahab, 2022), especially since the region is characterized by minimal cloud cover, primarily limited to winter and spring seasons (Al-Ramahy *et al.,*

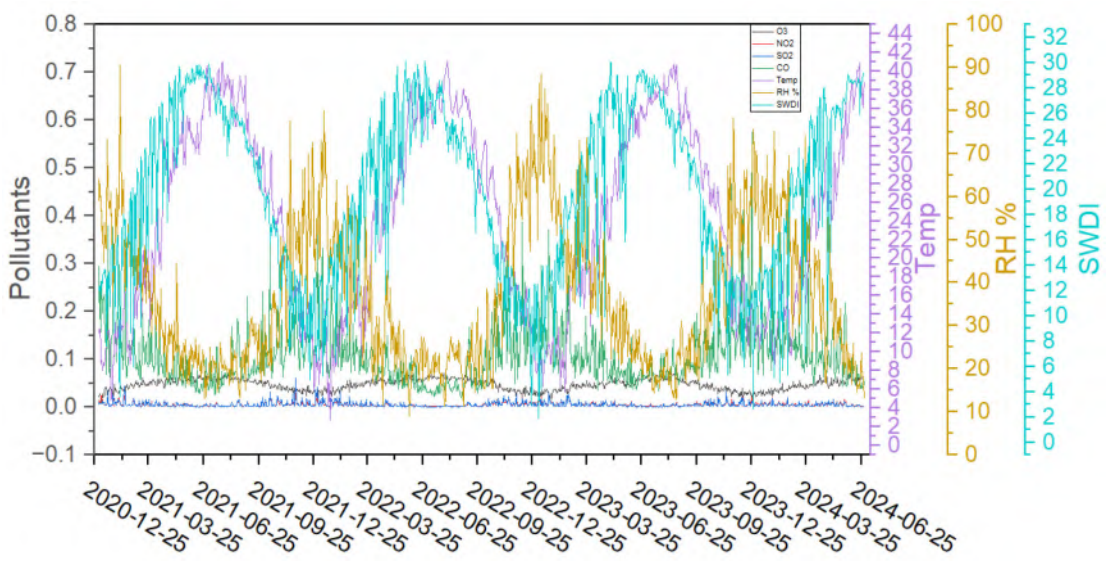

Fig. 2: Time series of PC1 elements

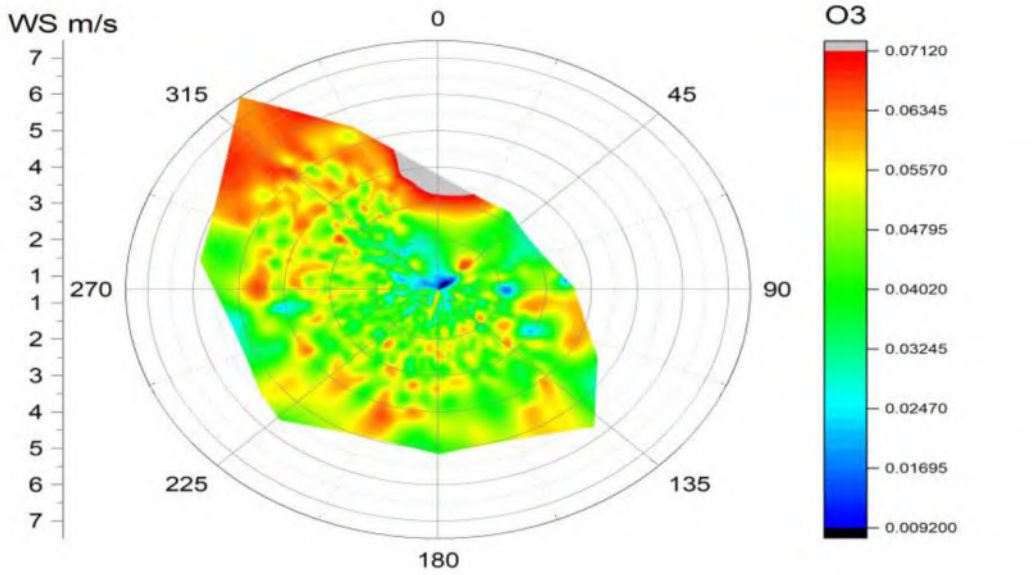

Fig. 3: Polar plot of PC1,WS and O_3

2022), and high temperatures (Al-Ataby and Altmimi, 2021). The negative loadings for primary pollutants (NO_2, SO_2, CO) suggest their consumption in these reactions, potentially forming ozone and other secondary pollutants. The negative correlation with relative humidity indicates that drier conditions favor these processes. The rise in O_3 concentrations coincides with T and SWDI, and vice versa is true with ozone precursors (NO_2, SO_2 and CO) (Fig. 2). In agricultural areas, this component might be influenced by biogenic volatile organic compound (VOCs) emissions from crops, which can participate in ozone formation (Nguyen *et al.,* 2022). The positive loadings of wind speed in desert suburb with 0.26 and industrial area with 0.27 suggests that pollutant dispersion and mixing play important roles in this setting. Fig. 3 polar plot (wind rose) shows that tropospheric ozone formation processes occur mostly in the northern and northwestern regions.

PC2, explaining 20-22% of the variance, primarily represents particulate matter dynamics with strong positive loadings for $PM_{2.5}$ (0.52-0.55) and PM_{10} (0.48-0.49) across all sites (Fig. 4). In addition to positive loadings of gases pollutants NO_2 (0.209-0.228) and SO_2 (0.240-0.304) with temperature (0.270-0.319). However, PC2 exhibits site-specific characteristics. In agricultural areas, PC2 highlights the role of thermal convection (temperature) in particulate concentrations, with practices like soil tillage and biomass burning contributing to emissions. Ammonia from fertilizers reacts with SO_2 and NO_2, forming secondary particulates. In urban park areas, PC2 shows the impact of the urban heat island effect (temperature) with vehicular emissions and dust contributing to particulates. NOx and SO_2 undergo photochemical aging, forming secondary aerosols. In desert suburban areas, PC2 emphasizes the role of wind-driven dust and long-range transport. Suburban development increases

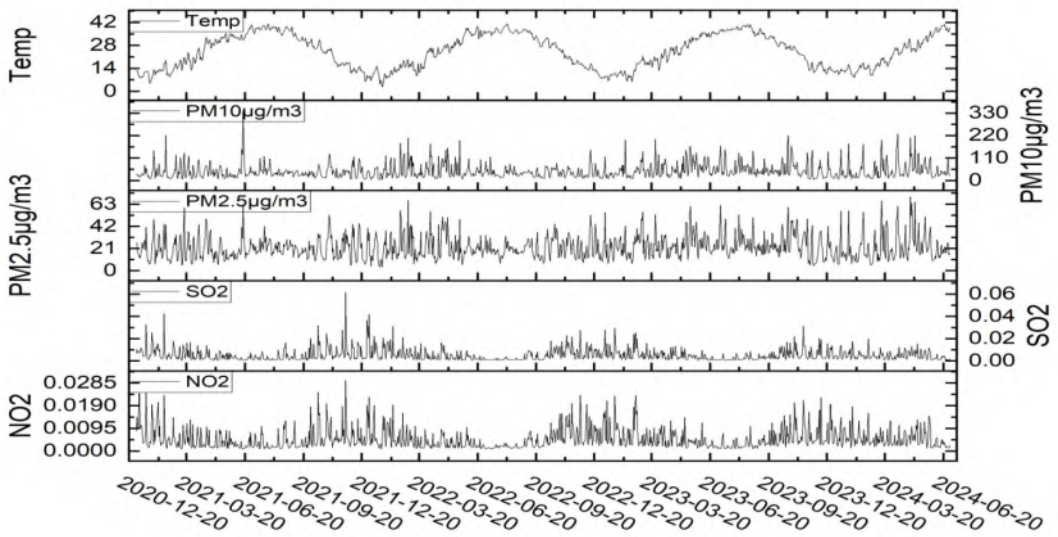

Fig. 4: Time series of PC2 elements PM, NO_2, SO_2 and temperature.

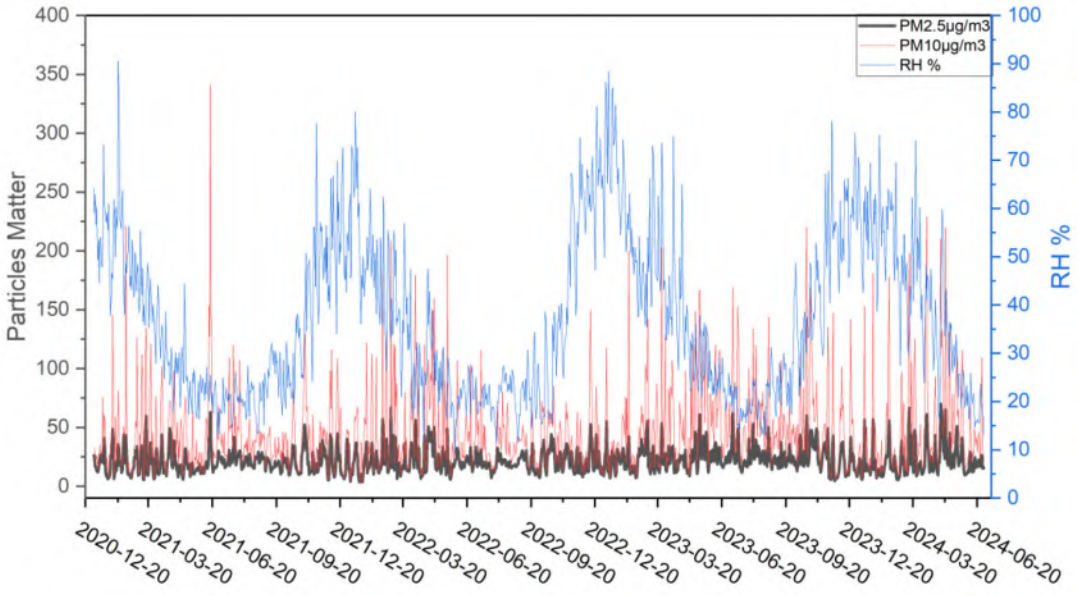

Fig. 5: Time series of PC3 elements, RH and PM (PM_{10} and $PM_{2.5}$).

local dust emissions, while weather patterns bring in aerosols from distant sources (Fig. 4). In industrial areas, PC2 reflects the impact of direct emissions from industrial processes, with SO_2 converting to sulfate aerosols. Temperature inversions and wind patterns lead to pollutant accumulation, while machinery and traffic resuspend dust. The positive relationship between temperature and PC1 in all regions and PC2 in the agricultural region, the park region, also the desert Suburb and the industrial region, although to a lesser degree, confirms the important role of increasing pollutant emissions, (Al-Knani *et al.,* 2021) reported, when studying the relationship between solar radiation and temperature, that temperature plays a decisive role in increasing air pollutants.

PC3 contributing 14-16% of the variance, consistently represents meteorological influences on particulate matters. It shows positive loadings for PM_{10} (0.47-0.49), $PM_{2.5}$ (0.35-0.38), relative humidity (0.35-0.37), and wind speed (0.36-0.42). The positive correlations between PM and RH can be explained by two factors. First, high RH absorbs solar radiation, lowering surface temperatures and reducing air currents, which leads to increased pollutant concentrations (Jayamurugan *et al.,* 2013). Second, high RH (above 80%) promotes the formation of fine particles, such as $CaSO_4 \cdot 2H_2O$ crystals, through the oxidation of SO_2 on calcium carbonate. In contrast, lower RH (below 40%) results in fewer crystal formations. This effect is most pronounced in winter when RH is highest (Yue *et al.,* 2022). Regarding wind speed, high winds stir up dust, indicating sandstorm potential, especially in agricultural areas near barren lands. In the park area, the PM_{10} load was higher (0.49), while wind speed had a lower impact compared to agricultural areas, suggesting that slower winds may increase PM

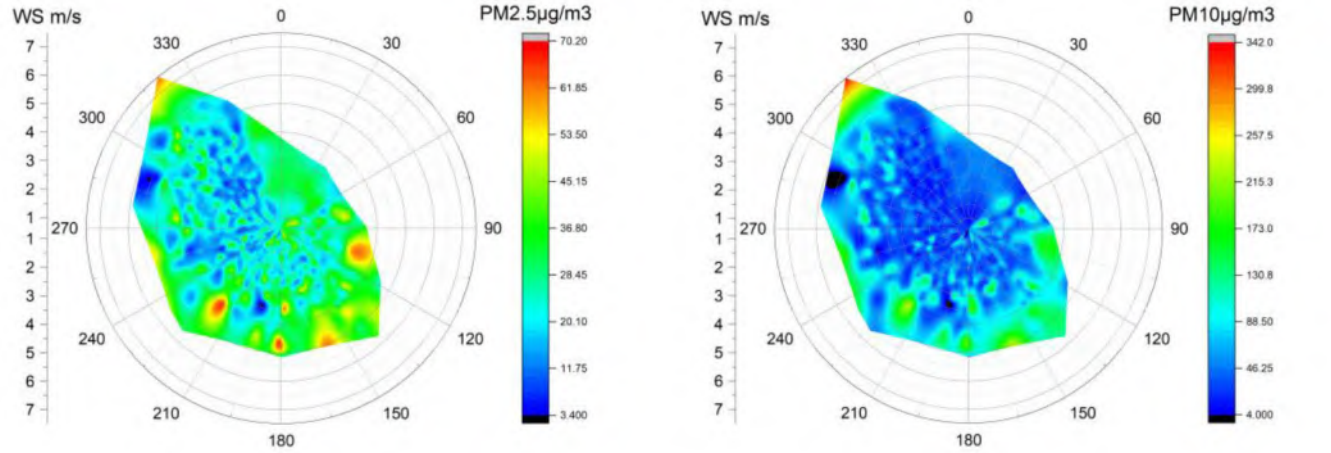

Polar plot of $PM_{2.5}$, WS and WD

Polar plot of PM_{10}, WS and WD

Fig. 6: Polar plot of PC2.

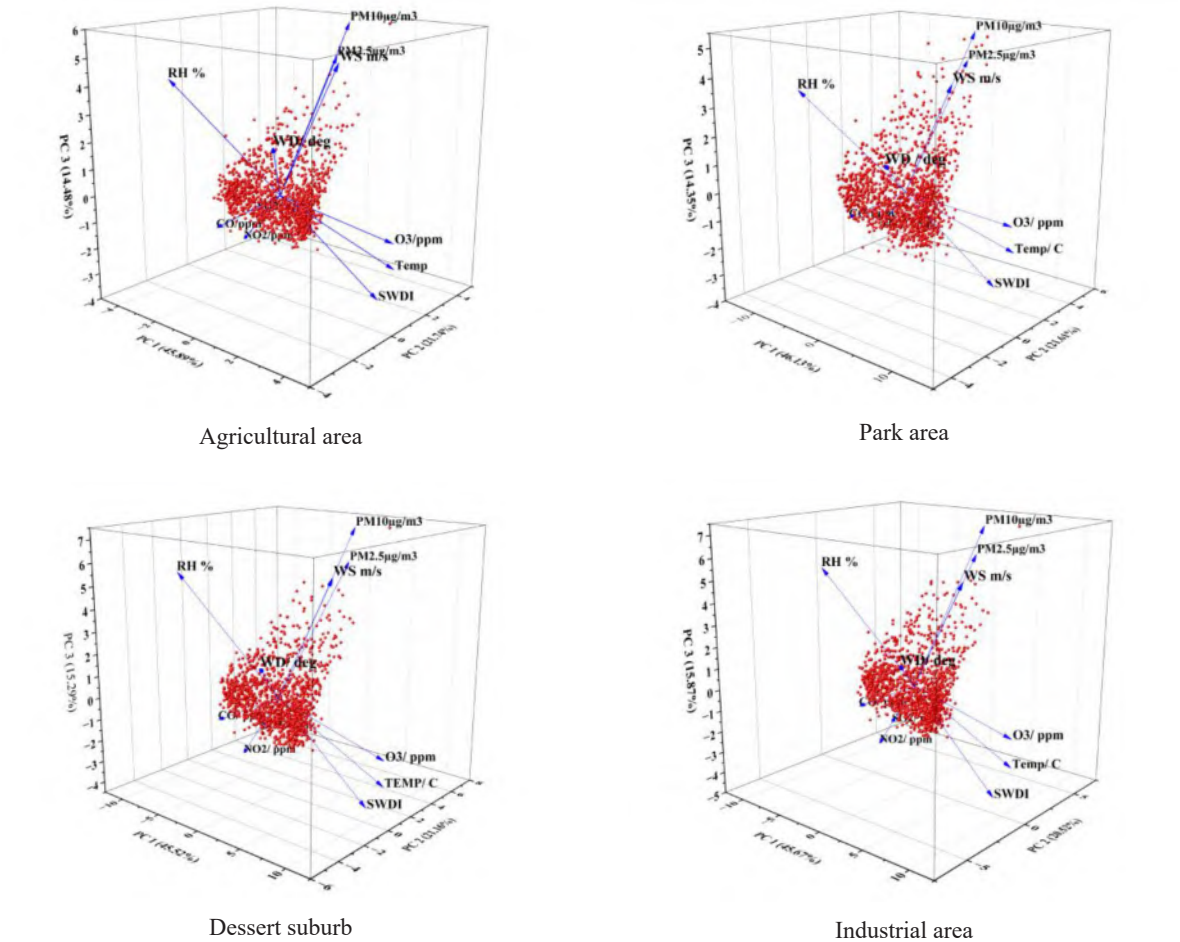

Agricultural area

Park area

Dessert suburb

Industrial area

Fig. 7: 3D Biplot of principal components.

concentrations, particularly from $PM_{2.5}$ and traffic emissions. This is more common in summer, where higher temperatures enhance convection and wind speeds. Fig. 5 shows elements of PC3 (RH, PM_{10} and $PM_{2.5}$). Fig. 6 polar plot of PC3 shows $PM_{2.5}$ concentrations more spread out at different speeds while PM_{10} are less spread out due to their heavier weight.

Analysis of the first three components (PC1, PC2 and PC3) across four distinct environments, agricultural areas, parks, desert suburbs and industrial areas, reveals complex interactions between anthropogenic emissions, photochemical processes, and

Table 3: Index of pollutants (IP) and their effects on AQI index

Locations	AQI index under different pollutants ((IP)											
	IP (O_3)		IP (NO_2)		IP (SO_2)		IP (CO)		IP ($PM_{2.5}$)		IP (PM_{10})	
	Days	%	Days	%	Days	%	Days	%	Days	%	Days	%
Agricultural area	184	14.4	0	0	0	0	0	0	1085	85.0	8	0.6
Park area	153	12.0	0	0	0	0	0	0	1121	87.8	3	0.2
Desert suburb	199	15.6	0	0	0	0	0	0	1074	84.1	4	0.3
Industrial area	162	12.7	0	0	0	0	0	0	1108	86.8	7	0.5

Table 4: The seasonal air quality index (AQI) in four areas under different categories

Location/ Area	Season	Good		Moderate		Unhealthy for sensitive groups		Unhealthy		Very unhealthy		Hazardous	
		day	%	day	%	day	%	day	%	day	%	day	%
Agricultural area	Winter	47	14.2	243	73.6	35	10.6	5	1.5	0	0	0	0
	Spring	15	4.1	284	77.2	57	15.5	12	3.3	0	0	0	0
	Summer	0	0	284	92.8	20	6.5	1	0.3	1	0.3	0	0
	Autmn	10	3.7	221	82.5	36	13.4	1	0.4	0	0	0	0
Total		72	5.6	1037	81.2	148	11.6	19	1.5	1	0.1	0	0
Park area	Winter	40	12.1	256	77.3	32	9.7	3	0.9	0	0	0	0
	Spring	14	3.8	291	79.1	55	14.9	8	2.2	0	0	0	0
	Summer	0	0	291	95.1	14	4.6	1	0.3	0	0	0	0
	Autmn	8	2.9	233	85.3	31	11.4	1	0.4	0	0	0	0
Total		61	4.8	1071	83.9	132	10.3	13	1	0	0	0	0
Desert suburb	Winter	57	17.3	238	72.1	31	9.4	4	1.2	0	0	0	0
	Spring	18	4.9	282	76.6	59	16	9	2.4	0	0	0	0
	Summer	0	0	286	93.5	18	5.9	1	0.3	1	0.3	0	0
	Autmn	14	5.1	233	85.3	24	8.8	2	0.7	0	0	0	0
Total		89	7	1039	81.4	132	10.3	16	1.3	1	0.1	0	0
Industrial area	Winter	43	13.1	250	76.0	32	9.7	4	1.2	0	0	0	0
	Spring	16	4.3	285	77.2	58	15.7	10	2.7	0	0	0	0
	Summer	0	0	280	91.5	24	7.8	1	0.3	1	0.3	0	0
	Autmn	8	2.9	236	86.4	28	10.3	1	0.4	0	0	0	0
Total		67	5.2	1051	82.3	142	11.1	16	1.3	1	0.1	0	0

atmospheric dynamics. Fig. 7 shows three-dimensional 3D Biplot of air pollutants and meteorological elements loadings.

Air quality index (AQI)

The impact of the IP (O_3) on the AQI ranged from 12% in the park area, corresponding to 153 days, to 15.6% in the desert suburb, accounting for 199 days, it is usually in summer and spring and to a lesser extent in winter and autumn seasons (Fig. 8). Table 3 contains the index of each pollutant and the number of days of its impact on AQI in all areas. IP ($PM_{2.5}$) shows a much stronger influence on the AQI, with its impact ranging from 84.1% of the study days in the desert suburb to approximately 87.8% in the park area. This indicates that $PM_{2.5}$ is the predominant driver of air quality deterioration in these areas. IP (PM_{10}) had a minimal impact on the AQI, ranging between 0.2% to 0.6%, corresponding to only 3-8 days. This limited influence is likely due to sporadic dust storms, as PM_{10} is primarily composed of larger particles, including dust and aerosols. Regarding to IP (NO_2, SO_2, CO), shows no significant impact on the AQI.

Table 4 categorizes AQI into six levels, from "Good" to "Very dangerous," showing the number and percentage of days each category occurred in each area. In winter, all areas generally have the best air quality. The agricultural area records the highest percentage of "Good" days (14.2%), while the desert suburb has the greatest number of "Good" days (57 days, 17.3%). However, there are still some "Unhealthy" days, particularly in the agricultural area (1.5%). In spring, there is a notable increase in "Unhealthy for sensitive groups" days across all areas, with the desert suburb having the highest percentage (16%). "Moderate" air quality is predominant in spring, ranging from 76.6% to 79.1%, while the

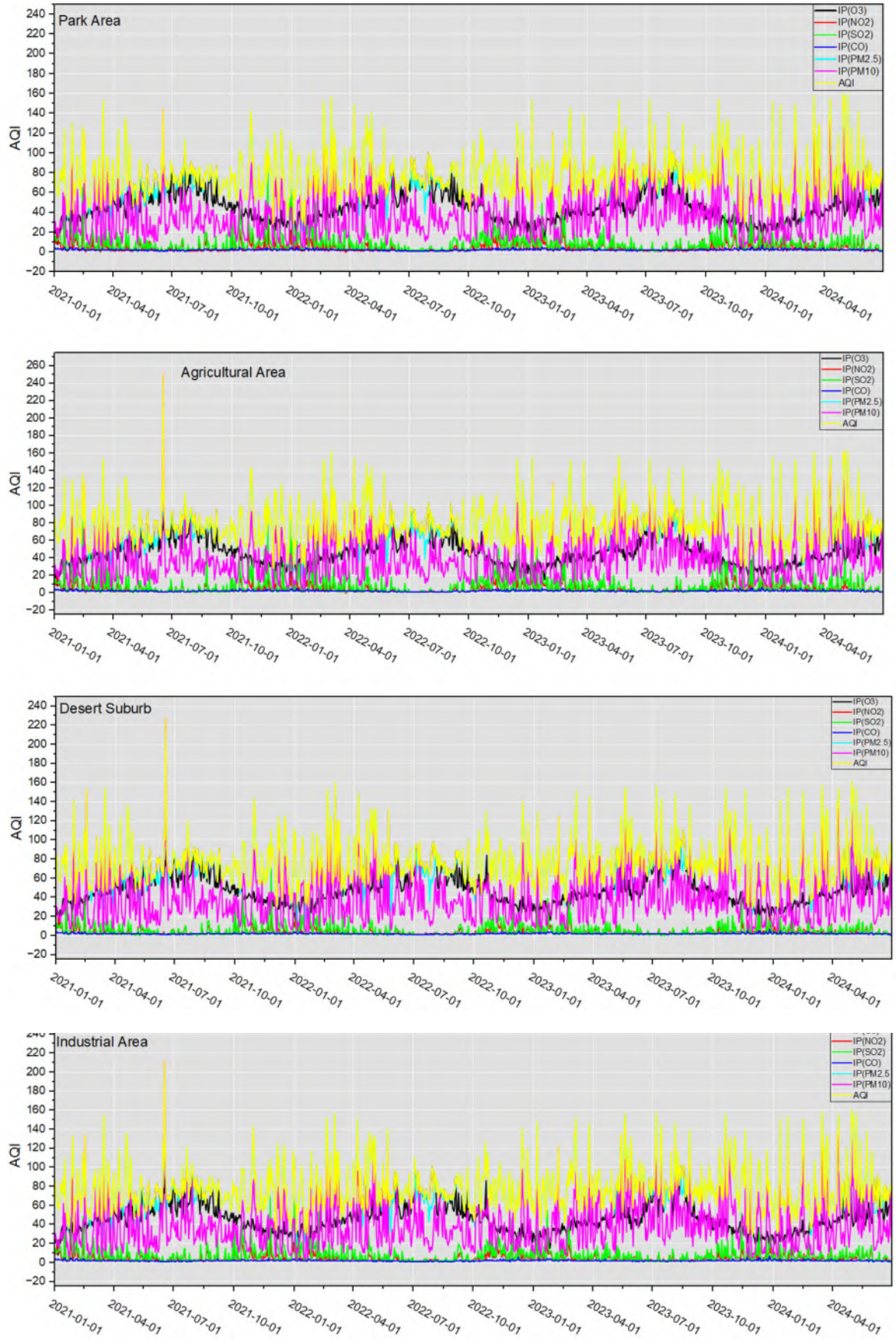

Fig. 8: AQI and IP (O_3, NO_2, SO_2, CO, $PM_{2.5}$ and PM_{10}) of four Areas.

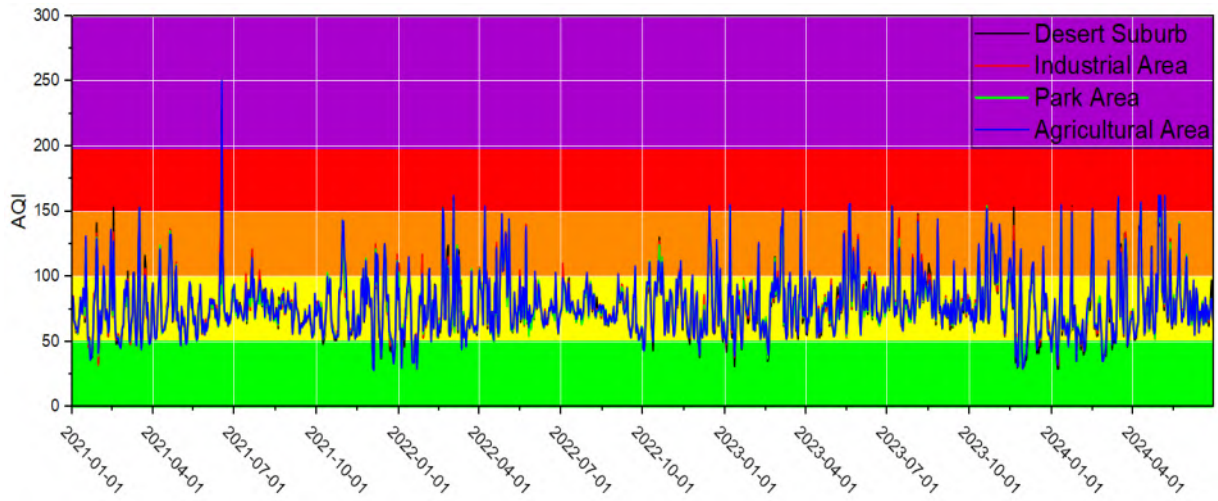

Fig. 9: Time series of the air quality index (AQI).

Industrial Area records the highest percentage of "Unhealthy" days (2.7%). In summer, "Moderate" air quality days dominate, with no "Good" days recorded in any area. Each of the agricultural area, desert suburb, and industrial area records one "Very unhealthy" day (0.3%). The park area maintains the highest percentage of "Moderate" days (95.1%) during summer. In autumn, air quality improves compared to summer, with some return of "Good" days. The desert suburb has the highest percentage of "Good" days in autumn (5.1%), while "Moderate" air quality still dominates (82.5%-86.4%). The agricultural area shows the highest variability in air quality across seasons, with the highest percentage of "Unhealthy for Sensitive groups" days in spring (15.5%) and the most significant improvement in "Good" days from summer to autumn. The park area maintains the most consistent air quality throughout the year, with the lowest percentage of "Unhealthy" days (1%) and no "Very unhealthy" days. The desert suburb has the best overall air quality, with the highest total percentage of "Good" days (7%) and the most significant seasonal variation in "Good" days. Conversely, the industrial area exhibits the poorest overall air quality, with the lowest percentage of "Good" days (5.2%) and the highest percentage of "Unhealthy" days (1.3%), showing the least improvement from summer to autumn.

Fig. 9 shows the time series of the air quality index (AQI) for the four areas under study, The majority of the days studied were classified as having moderate air quality, which is normal for such areas, and therefore the air quality is not bad for a large group of people except those who suffer from very severe respiratory diseases.

CONCLUSIONS

The study used principal component analysis to identify three main factors influencing air pollution: photochemical smog formation (45-46% variance), particulate matter dynamics (20-22%), and meteorological influences on particulates (14-16%). The air quality index analysis revealed $PM_{2.5}$ as the primary driver of air quality deterioration (84-88% of days), followed by ozone (12-16%). Seasonal variations showed winter with the best air quality, summer with no "Good" days, and autumn improving. Among the areas studied, the desert suburb had the best overall air quality, while the industrial area had the poorest and these results indicate that air quality is not ideal but not significantly dangerous, requiring strategies to improve AQI levels to ensure a better air environment.

ACKNOWLEDGEMENT

The authors would like to thank the Ministry of Environment, the Karbala Environment Directorate for their access to the data of pollutants monitored through their devices.

Conflict of Interests: The authors declare that there is no conflict of interest related to this article.

Funding: The authors did not receive support from any organization for the submitted work.

Data availability: O_3, NO_2, SO_2, CO, $PM_{2.5}$ and PM_{10} data for January 2021 – June 2024 were obtained from Copernicus at: https://ads.atmosphere.copernicus.eu/cdsapp#!/dataset/cams-europe-air-quality-forecasts?tab=form. Meteorological data, including T, RH, SWDI, WS, and WD, were obtained from NASA's (POWER), Agroclimatology data at: https://power.larc.nasa.gov/data-access-viewer/. All data cover the period from January 2021 - June 2024.

***Author contribution*: H. H. Ali:** Data checked, processed, analyzed, and presented, Investigation, Writing-original draft; **B. I. Wahab:** Supervision, writing review, and editing; **H. M. Abdul-Hmeed:** Supervision.

Disclaimer: The contents, opinions and views expressed in the research article published in the Journal of Agrometeorology are the views of the authors and do not necessarily reflect the views of the organizations they belong to.

Publisher's Note: The periodical remains neutral with regard to jurisdictional claims in published maps and institutional affiliations.

REFERENCES

Abdullatif, R., Hammadi, S. R. and Alsaady, Q. (2021). Air Quality Analyses in the City of Karbala, Iraq. Paper presented at the IOP Conference Series: Materials Science and Engineering, 1184: 012014. http://doi.org/10.1088/1757-899X/1184/1/012014

Al-Ataby, I. K. and Altmimi, A. I. (2021). Testing the relationship between air temperature and relative humidity by using t-test for some selected stations in iraq. *Al-Mustansiriyah J. Sci.,* 32(2): 1-7. http://doi.org/10.23851/mjs.v32i2.975

Al-Ramahy, Z. A., Nassif, W. G. and Al-Taai, O. T. (2022). Impact of Clouds (High, Medium and Low) on Blocking of Solar Radiation over ifferent Regions in Iraq D. *Indian J. Ecol*., 49(18): 334-343. https://indianecologicalsociety.com/conferences/

Al-Knani, B. A., Abdulkareem, I. H., Nemah, H. A. and Nasir, Z. (2021). Studying the Changes in Solar Radiation and Their Influence on Temperature Trend in Iraq for a Whole Century. *Baghdad Sci. J.,* 18(2): 1076-1076. http://dx.doi.org/10.21123/bsj.2021.18.2(Suppl.).1076

Al-Samarrai, H. M. and Al-Jiboori, M. H. (2022). Estimation of the Daily Maximum Air Temperature for Baghdad City Using Multiple Linear Regression. *Al-Mustansiriyah J. Sci.,* 33(4): 9-14. http://doi.org/10.23851/mjs.v33i4.1168

Anad, A. M., Hassoon, A. F. and Al-Jiboori, M. H. (2022). Assessment of air pollution around Durra refinery (Baghdad) from emission NO2 gas at April Month. *Baghdad Sci. J.,* 19(3): 0515-0515. http://dx.doi.org/10.21123/bsj.2022.19.3.0515

Birinci, E., Denizoğlu, M., Özdemir, H., Özdemir, E. T. and Deniz, A. (2023). Ambient air quality assessment at the airports based on a meteorological perspective. *Environ. Monit. Assess.,* 195(12): 1542. https://doi.org/10.1007/s10661-023-12135-3

Byrwa-Hill, B. M., Venkat, A., Presto, A. A., Rager, J. R., Gentile, D. and Talbott, E. (2020). Lagged association of ambient outdoor air pollutants with asthma-related emergency department visits within the Pittsburgh region. Intern. *J. Environ. Res. Public Health*, 17(22): 8619. https://doi.org/10.3390/ijerph17228619

Gayer, A., Adamkiewicz, Ł., Mucha, D., and Badyda, A. (2018). Air quality health indices-review. Paper presented at the MATEC Web of Conferences. Fire and Environmental Safety Engineering 2018 (FESE 2018), 00002: 8. https://doi.org/10.1051/matecconf/201824700002

Jadem, A. M., Jasem, I. M. and Al-Ramahi, F. K. (2023). Monitoring Pollution and the Trend of Air Quality in Brick Factories in the Nahrawan Region and its Impact on Baghdad, Using Remote Sensing Data. *Ibn Al-Haitham J. Pure Appl. Sci.,* 36(4): 51-62. https://doi.org/10.30526/36.4.3162

Jayamurugan, R., Kumaravel, B., Palanivelraja, S. and Chockalingam, M. P. (2013). Influence of Temperature, Relative Humidity and Seasonal Variability on Ambient Air Quality in a Coastal Urban Area. *Intern. J. Atmos. Sci.,* 2013: 7. https://doi.org/10.1155/2013/264046

Mohamed, M. A. E.-H., Hwehy, M. M. A., Moursy, F. I. and El-Tantawi, A. M. (2023). The synergy of ambient air quality and thermal discomfort: A case study of Greater Cairo, Egypt. *J. Agrometeorol.*, 25(4): 553–559. https://doi.org/10.54386/jam.v25i4.2309

Namrata, Jariwala and Drashti, Kapadia. (2021). Statistical analysis of tropospheric ozone and its precursors using principal component analysis in an urban area of Surat, India. *Adv. Environ. Tech.,* 1: 1-10. https://doi.org/10.22104/aet.2021.4834.1308

Nguyen, D.-H., Lin, C., Vu, C.-T., Cheruiyot, N. K., Nguyen, M. K., Le, T. H., Lukkhasorn, W., Vo, T., -D., -H., Bui, X., -T. (2022). Tropospheric ozone and NOx: A review of worldwide variation and meteorological influences. *Environ. Tech. Innov.,* 28: 102809. https://doi.org/10.1016/j.eti.2022.102809

Pandey, V. (2018). The discomfort levels in Gujarat-A comparison of different thermal stress indices. *J. Agrometeorol*., 20(1): 1-10. https://doi.org/10.54386/jam.v20i1.494

Shihab, A. S. (2021) Assessment of ambient air quality of Mosul city/Iraq via Air Quality Index. J. Ecol. Eng., 22(10): 241-250. https://doi.org/10.12911/22998993/142448

Taghizadeh, F., Mokhtarani, B. and Rahmanian, N. (2023). Air pollution in Iran: The current status and potential solutions. *Environ. Monit. Assess.*, 195(6): 737. https://doi.org/10.1007/s10661-023-11296-5

Wahab, B. (2022) Estimation of ozone content employing ground-based UV measurements over Baghdad City, Iraq. *Caspian J. Environ. Sci.,* 20(4): 747-755. https://doi.org/10.22124/CJES.2022.5758

Yaseen, A. H. and Abdulkareem, A. K. (2022). Treatment Missing Data of Daily and Monthly Air Temperature in Some Iraqi cities by Using Curve Fitting. *Al-Mustansiriyah J. Sci.,* 33(4): 34-41. https://doi.org/10.23851/mjs.v33i4.1202

Yue, y.,Cheng, J., Soo Lee, K., Stocker, R., He, X., Yoa, M. and Wang, J. (2022). Effects of relative humidity on heterogeneous reaction of SO2 with $CaCO_3$ particles and formation of $CaSO_4 \cdot 2H_2O$ crystal as secondary aerosol. *Atmos. Environ.,* 268: 118776. https://doi.org/10.1016/j.atmosenv.2021.118776

Zuśka, Zbigniew., Kopcińska, Joanna., Dacewicz, Ewa., Skowera, Barbara., Wojkowski, Jakub., Wojtaszek, Agnieszka Ziernicka. (2019). Application of the Principal Component Analysis (PCA) Method to Assess the Impact of Meteorological Elements on Concentrations of Particulate Matter (PM10): A Case Study of the Mountain Valley (the Sącz Basin, Poland). *Sustainability*, 11: 6740. https://doi.org/10.3390/su11236740